Mendeleev Communications

Mendeleev Commun., 2025, **35**, 35–38

Influence of the anion ratio in the composition of mixed benzoate/pentafluorobenzoate complexes of europium on the structure and photoluminescent properties

Maxim A. Shmelev,*[a] Anastasia A. Levina,[b] Aleksandr S. Chistyakov,[a] Evgeniya A. Varaksina,[c] Julia K. Voronina,[a] Galina A. Razgonyaeva,[a] Ilya V. Taydakov,[c] Alexey A. Sidorov[a] and Igor L. Eremenko[a]

[a] *N. S. Kurnakov Institute of General and Inorganic Chemistry, Russian Academy of Sciences, 119991 Moscow, Russian Federation. E-mail: shmelevma@yandex.ru*
[b] *N. D. Zelinsky Institute of Organic Chemistry, Russian Academy of Sciences, 119991 Moscow, Russian Federation*
[c] *P. N. Lebedev Physical Institute, Russian Academy of Sciences, 119991 Moscow, Russian Federation*

DOI: 10.71267/mencom.7566

Mixed carboxylate benzoate (bz)/pentafluorobenzoate (pfb) complexes with different ratios of pfb and bz anions in the $\{Eu(EtOH)_2(pfb)(bz)_2\}_n$ and $\{Eu(EtOH)(pfb)_2(bz)\}_n$ compositions were obtained and structurally characterized. Changes in the pfb/bz ratio lead to changes in the geometry of the polymer chains and the lanthanide polyhedron, as well as to a rearrangement of the system of non-covalent interactions, which also affects the photoluminescent properties. The synthesized compounds were characterized by X-ray diffraction study, IR spectroscopy and CHN analysis; non-covalent interactions were analyzed using Hirshfeld surface analysis.

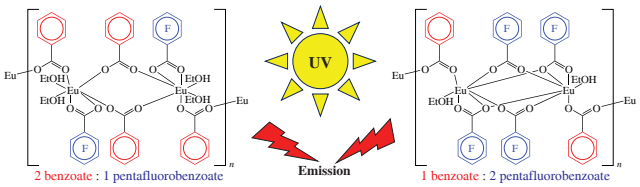

Keywords: europium(III), mixed carboxylate complexes, pentafluorobenzoate, benzoate, non-covalent interactions, photoluminescence, Hirshfeld surface analysis.

Lanthanide complexes are utilized across various fields, including in lasers and lighting systems, electroluminescent devices, diodes, and sensors, as well as for biomedical imaging due to their photoluminescent properties.[1–8] An important practical challenge is to develop methods for synthesizing lanthanide coordination compounds with optimal photoluminescent characteristics. One effective approach to purposefully improve photoluminescent characteristics is the preparation of multi-ligand lanthanide compounds. Previous works have demonstrated that the simultaneous coordination of multiple organic ligands with lanthanide ions leads to a significant increase in luminescence efficiency by altering the metal ion polyhedra geometry, reducing interactions between ions, and decreasing conformational changes.[9–13] Studies on europium compounds have shown that the simultaneous combination of four anionic ligands in the complex can lead to a fivefold increase in luminescence efficiency.[14] Nevertheless, the structure of the resulting compounds was not therein established and no investigations on the ratio of ligands in the composition of the compounds influences on the structure and photoluminescent properties were carried out, which does not fully reveal the factors affecting the properties of the resulting compounds.

In our research, we examined the structure and photoluminescent properties of mixed carboxylate benzoate/pentafluorobenzoate (bz/pfb) europium complexes with different anion ratios. The simultaneous incorporation of fluorinated and non-fluorinated aromatic ligands into the compound leads to the formation of a range of different non-covalent interactions among the organic ligand molecules (*e.g.*, π···π, C–F···π, and C–H···F). These interactions can significantly influence not only the molecular and crystalline structure but also the photoluminescent properties of the resulting compounds.[15–19]

In this work, new mixed carboxylate compounds, $\{Eu(EtOH)_2(pfb)(bz)_2\}_n$ **1** and $\{Eu(EtOH)(pfb)_2(bz)\}_n$ **2**, were prepared by the disproportionation reaction between europium pentafluorobenzoate and europium benzoate in ethanol (Scheme 1, see also Online Supplementary Materials, Scheme S1). The composition of resulting mixed carboxylate compounds **1** and **2** was determined based on the ratio of the initial europium salts (pfb/bz was 1 : 2 or 2 : 1). The structures of

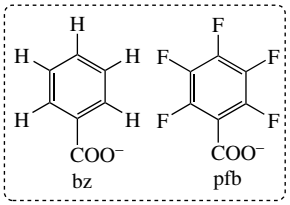

$$[Eu(H_2O)_5(pfb)_3] + 2[Eu(H_2O)_4(bz)_3] \xrightarrow{EtOH} \{Eu(EtOH)_2(pfb)(bz)_2\}_n \quad \mathbf{1}$$

$$2[Eu(H_2O)_5(pfb)_3] + [Eu(H_2O)_4(bz)_3] \xrightarrow{EtOH} \{Eu(EtOH)(pfb)_2(bz)\}_n \quad \mathbf{2}$$

Scheme 1

compounds **1** and **2** were studied by single-crystal X-ray diffraction analysis,† while the phase purity of the synthesized products was confirmed by X-ray powder diffraction analysis (Figures S1 and S2) and CHN analysis.

Compound **1** consists of mononuclear fragments $\{Eu(EtOH)_2(pfb)(bz)_2\}$, with all benzoate anions involved in bridging the lanthanide atoms to form a 1D polymer chain (Figure 1). The distances between neighboring europium ions in the chain are 4.980(7) and 4.893(6) Å. Each europium atom is chelated by the pfb anion, and the coordination environment of the metal center is completed by two ethanol molecules, forming a triangular dodecahedron (Table S1). The elementary unit of coordination polymer **2** is a binuclear fragment consisting of two europium ions linked by four pentafluorobenzoate anions, with anions acting as bridges and the other two serving as chelate bridges. The polymer chain is formed *via* two bz anions linking dimer fragments. Additionally, each europium ion coordinates with a single ethanol molecule, completing its coordination environment as a triangular dodecahedron. The distance between europium ions within an elementary unit is 3.994(1) Å, while the distance between chains is 5.374(2) Å.

When considering the chain structure relative to the planes formed by the metal ions, it is observed that in the equatorial plane of complex **1**, the pfb anions and ethanol molecules are linked by classical hydrogen bonds of the O–H···O type. The bz fragments occupy the axial positions, with their aromatic rings rotated at an angle of 102.6(2)° preventing the formation of C–H···π interactions due to the significant distance between them. In the chain of complex **2**, only ethanol molecules are placed in the equatorial plane, while all aromatic fragments of the coordinated anions are located above and below the plane. This arrangement leads to π···π interactions between the aromatic fragments of the bz and the chelating bridging pfb anions, with distances between the planes and centroids of the rings being approximately 3.4 and 4.0 Å. Due to the mutual arrangement of the anions, the pfb ring shifts relative to the bz ring, creating an additional overlap with the carboxy group of the bz anion at a minimum distance of 3.242(2) Å. The polymeric chains of complexes **1** and **2** are further stabilized by a series of hydrogen bonds between the OH groups of coordinated EtOH molecules and the oxygen atoms of the carboxyl groups, as well as C–F···π interactions (Table S2).

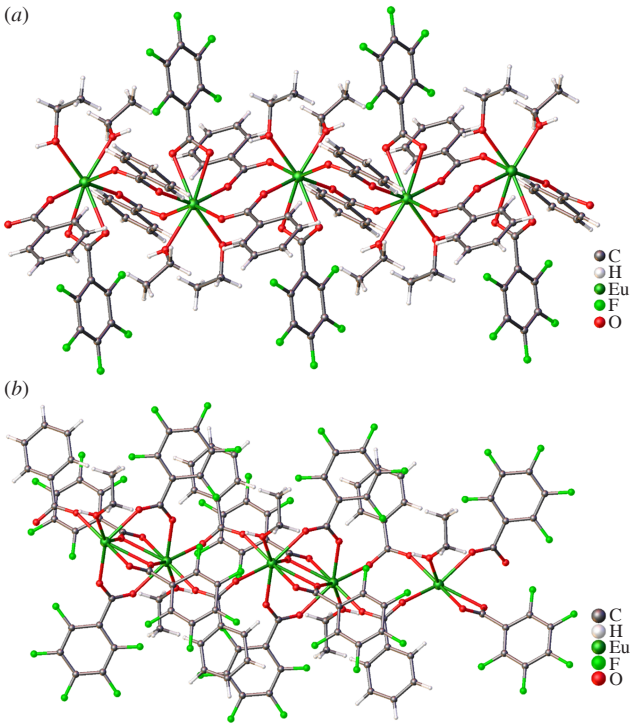

Figure 1 Fragment of the polymer chains in (*a*) complex **1** and (*b*) complex **2**.

Analysis of the CCDC (CSD version 5.45 Nov. 2023) revealed that the previously described benzoate[26] $\{Eu(MeOH)_2(bz)_3\}_n$ and pentafluorobenzoate[27] $\{Eu(EtOH)_2(pfb)_3\}_n$ polymers, along with compound **1** we obtained, have a similar structure. However, the structure of compound **2** differs from the previously reported homoanionic analogs. Thus, varying the ratio of carboxylate anions in bz/pfb compounds **1** and **2** led to an unexpected structural transformation in comparison to the bz and pfb polymers.

The crystal packing of complex **1** is stabilized by intermolecular C–F···π and O–H···O non-covalent interactions (Table S3). Increasing the number of benzoate anions in complex **2** leads to the formation of C–H···F and C–H···O interactions, consistent with the Hirshfeld surface analysis data. The main contributions to the stabilization of the Hirshfeld surface in the polymer chain fragment of complex **1** consist of F···H (28.5%), O···H (13.1%), and C···F (3.0%) interactions. In the polymer chain fragment of complex **2**, there is a decrease in the proportion of O···H (6.8%) and an increase in F···H (34.8%), C···F (9.6%), and F···F interactions (from 0.6% in complex **1** to 13.0% in complex **2**). The contribution of C···C interactions in both complexes remains below 3%.

The photophysical properties of polymers $\{Eu(EtOH)_2(pfb)(bz)_2\}_n$ **1** and $\{Eu(EtOH)(pfb)_2(bz)\}_n$ **2** with different pfb/bz ratios were investigated using steady-state and time-resolved luminescence studies (Table 1). Figure 2 shows the photoluminescence spectra of the complexes at 77 K upon ligand excitation at 280 nm. The characteristic narrow

† *Crystal data for* **1**. $C_{25}H_{22}EuF_5O_8$ (M = 697.38), T = 296 K, triclinic space group $P\bar{1}$, a = 9.617(12), b = 12.176(14) and c = 12.357(9) Å, α = 100.90(4)°, β = 98.28(4)°, γ = 111.14(4)°, V = 1289(2) Å^3, Z = 2, μ(MoKα) = 2.516 mm^{-1}. At the angles 2.180 < θ < 24.707°, total of 8015 reflections were measured, including 4328 unique reflections (R_{int} = 0.0543) and 3679 reflections with $I > 2\sigma(I)$, which were used in all calculations. The final R_1 = 0.0790, wR_2 = 0.1305 (all data) and R_1 = 0.0647, wR_2 = 0.1256 [$I > 2\sigma(I)$], GOOF = 1.085. Largest diff. peak/hole 2.516 and –2.254 eÅ^{-3}.

Crystal data for **2**. $C_{23}H_{11}EuF_{10}O_7$ (M = 741.28), T = 100 K, triclinic space group $P\bar{1}$, a = 8.666(3), b = 10.616(3) and c = 14.094(3) Å, α = 76.802(10)°, β = 76.175(11)°, γ = 71.539(12)°, V = 1177.7(6) Å^3, Z = 2, μ(MoKα) = 2.788 mm^{-1}. At the angles 2.051° < θ < 26.000°, total of 8387 reflections were measured, including 4538 unique reflections (R_{int} = 0.0542) and 3939 reflections with $I > 2\sigma(I)$, which were used in all calculations. The final R_1 = 0.0563, wR_2 = 0.1140 (all data) and R_1 = 0.0467, wR_2 = 0.1085 [$I > 2\sigma(I)$], GOOF = 1.050. Largest diff. peak/hole 1.811 and –2.008 eÅ^{-3}.

The single crystal X-ray diffraction analysis was performed on a Bruker D8 Venture diffractometer equipped with a CCD detector (MoKα, λ = 0.71073 Å; CuKα, λ = 1.54178 Å, graphite monochromator). A semi-empirical absorption correction using the SADABS[20] program was applied to all compounds. Using Olex2,[21] the structure was solved with a ShelXS structure solution program using Direct Methods and refined using a ShelXL[22] refinement package with the Least Squares minimization in anisotropic approximation for nonhydrogen atoms. The H-atoms were added in the calculated positions and refined using the riding model in isotropic approximation. The geometry of metal polyhedra was determined using the program SHAPE 2.1.[23] The Hirshfeld surface was analyzed using the Crystal Explorer 17 program to evaluate the contribution of various non-covalent interactions to the crystal packings of the resulting complexes.[24,25]

CCDC 2361321 (**1**) and 2361322 (**2**) contain the supplementary crystallographic data for this paper. These data can be obtained free of charge from The Cambridge Crystallographic Data Centre *via* https://www.ccdc.cam.ac.uk.

Table 1 Radiative (A_{rad}) and nonradiative (A_{nrad}) decay rates, lifetimes (τ^{obs}), and intrinsic quantum yields (Q_{Ln}^{Ln}) of complexes **1** and **2**.

Compound	A_{rad}/s^{-1}	A_{nrad}/s^{-1}	τ^{obs}/ms		Q_{Ln}^{Ln} (%)
			T = 300 K	T = 77 K	
1	380	1010	0.715	0.700	27
2	380	800	0.850	1.485	32

luminescence bands correspond to the $^5D_0$–^7F_J (J = 0–4) transitions of the Eu^{3+} ion. An intense broad luminescence band is observed in the spectral range 27 000–16 000 cm^{-1} in the emission spectrum of complex **1**. Probably, the significant changes in molecular geometry due to the varying pfb/bz ratio lead to alterations in intermolecular interactions and the appearance of charge transfer states. Furthermore, the observed broad bands may also include the phosphorescence bands of the ligands.[29]

It is noteworthy that this band is absent at the room-temperature spectra (Figure S3). Nevertheless, the position and relative intensity of the f–f bands at both excitation and emission spectra of complexes **1** and **2** remain almost unchanged when the temperature decreases. This indicates that the structure of the complexes remains unchanged upon cooling, and therefore the disappearance of the broad band in the emission spectrum of complex **1** may be due to the enhancement of quenching processes at room temperature. This distinguishes investigated compounds from the previously studied heteronuclear complexes with carboxylates, whose broad luminescence bands are clearly visible in the emission spectra even at room temperature.[29,30] This observation once again confirms the insignificant influence of quenching processes on the luminescence efficiency in heteronuclear compounds.

The excitation spectra of complexes **1** and **2** at 77 and 300 K are shown in Figures S4 and S5, respectively. These spectra exhibit a broad band in the high-frequency range (up to 35 000 cm^{-1}) attributed to singlet–singlet excitation of the ligands, along with line-like bands corresponding to the f–f transitions of the Eu^{3+} ion. A low-intensity broad shoulder is observed in the 35 000–28 000 cm^{-1} range, likely corresponding to a charge transfer transition. The efficiency of energy transfer processes was estimated using calculations of the intrinsic quantum yield of luminescence *via* the Werts equation:[31]

$$Q_{Ln}^{Ln} = \frac{A_{rad}}{A_{rad} + A_{nrad}},$$

where A_{rad} and A_{nrad} are radiative and nonradiative rates constants, respectively. The unique energy spectra of the europium ion allow the calculation of the rates constants to be simplified. The dipole strength of the magnetic dipole transition $^5D_0$–$^7F_1$ does not depend on the ligand field environment in the first approximation, and radiative rate constant of the transition A_{01} is 14.65 s^{-1}. Therefore, the radiative rate constant can be calculated by the formula

$$A_{rad} = A_{01} n^3 \frac{I_{tot}}{I_{01}},$$

where I_{tot}/I_{01} is the ratio of the total area of the Eu^{3+} emission spectrum to the area of the magnetic dipole band. The obtained photophysical properties are presented in Table 1. The investigated compounds show a high rate of nonradiative decay, which could be attributed to relaxation through high-frequency vibrations of the C–H and O–H bonds in ethanol molecules. Additionally, the quenching rate of the europium excited state $^5D_0$ in complex **1** is significantly higher due to the presence of two EtOH molecules in the inner coordination sphere of Eu^{3+}. C–H vibrations of the benzoate anions may also contribute to the multiphonon relaxation of the europium ion's excited state. The same reasons can lead to temperature quenching of ligand excited states, which is evident from the disappearance of the broad band in the emission spectrum of complex **1** at 300 K. When the pfb/bz ratio was changed to 2 : 1, the rate of the nonradiative process slightly decreased, which can be attributed to the reduced number of coordinated EtOH molecules in complex **2**.

Moreover, the broadband emission observed in the range of 27 000–16 000 cm^{-1}, particularly pronounced in complex **1**, may provide an additional channel for energy losses from the excited state of the europium ion. Considering the spectral overlap of this band with the line-like europium emission in the luminescence spectrum of complex **1**, these states may contribute to back energy transfer from the europium ion to the ligand states, leading to noticeable excitation quenching even at low temperatures.

In summary, varying the ratio of the initial salts of benzoic and pentafluorobenzoic acids leads to the formation of mixed carboxylic compounds $\{Eu(EtOH)_2(pfb)(bz)_2\}_n$ **1** and $\{Eu(EtOH)(pfb)_2(bz)\}_n$ **2** with different compositions, accompanied by significant restructuring of the polymer chain geometry. The variation in the pfb/bz ratios in compounds **1** and **2** results in notable changes to both the polymer chain geometry and the system of non-covalent interactions. The photoluminescent properties of the investigated compounds are strongly dependent on the pfb/bz ratio, which affects the number of coordinated solvent molecules and the occurrence of intraligand charge transfer states. Changing the pfb/bz ratio from 1 : 2 to 2 : 1 increased efficiency of metal-centered luminescence by reducing the probability of multiphonon relaxation of excited states as well as the elimination of quenching of europium luminescence by the charge transfer state.

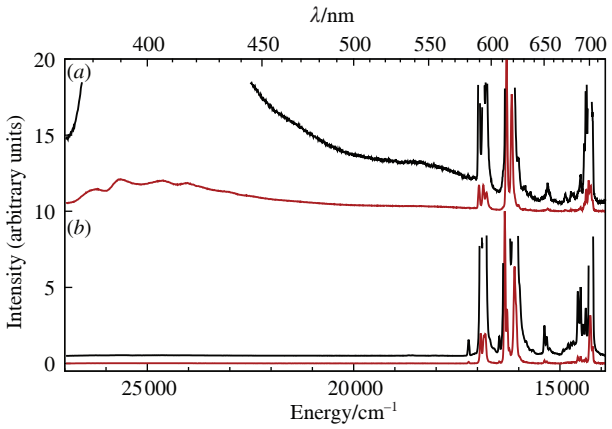

Figure 2 Emission spectra of (*a*) complex**1** and (*b*) complex **2** obtained at T = 77 K under excitation at λ_{ex} = 280 nm. The black line represents the spectra on an enlarged scale.

This work was supported by the Russian Science Foundation (grant no. 22-73-10192). IR spectroscopy, X-ray diffraction, powder X-ray diffraction, and CHN analyses of the complexes were performed using the equipment of the JRC PMR IGIC RAS as part of the state assignment of the IGIC RAS in the field of fundamental scientific research. Photophysical measurements were carried out with the financial support from the Ministry of Science and Higher Education of the Russian Federation, using the equipment of the Research Center for Molecular Structure Studies, INEOS RAS.

Online Supplementary Materials

Supplementary data associated with this article can be found in the online version at doi: 10.71267/mencom.7566.

References

1 Q. Zhang, S. O'Brien and J. Grimm, *Nanotheranostics*, 2022, **6**, 184; https://doi.org/10.7150/ntno.65530.

2 M. Wang, Y. Kitagawa and Y. Hasegawa, *Chem. – Asian J.*, 2024, **19**, e202400038; https://doi.org/10.1002/asia.202400038.

3 T. Xian, Q. Meng, F. Gao, M. Hu and X. Wang, *Coord. Chem. Rev.*, 2023, **474**, 214866; https://doi.org/10.1016/j.ccr.2022.214866.

4 B. Monteiro, J. Paulo Leal, R. F. Mendes, F. A. Almeida Paz, A. Linden, V. Smetana, A. V. Mudring, J. Avó and C. C. L. Pereira, *Mater. Chem. Phys.*, 2022, **277**, 125424; https://doi.org/10.1016/j.matchemphys.2021.125424.

5 D. Parker, J. D. Fradgley and K.-L. Wong, *Chem. Soc. Rev.*, 2021, **50**, 8193; https://doi.org/10.1039/D1CS00310K.

6 S. E. Bodmana and S. J. Butler, *Chem. Sci.*, 2021, **12**, 2716; https://doi.org/10.1039/D0SC05419D.

7 W. Bu, L. Wu, X. Zhang and A.-C. Tang, *J. Phys. Chem. B*, 2003, **107**, 13425; https://doi.org/10.1021/jp0356416.

8 D. O. Khristolyubov, D. M. Lyubov and A. A. Trifonov, *Russ. Chem. Rev*., 2021, **90**, 529; https://doi.org/10.1070/RCR4992.

9 N. V. Gogoleva, M. A. Shmelev, A. S. Chistyakov, G. A. Razgonyaeva, V. M. Korshunov, A. V. Tsorieva, I. V. Taydakov, A. A. Sidorov and I. L. Eremenko, *Mendeleev Commun.*, 2024, **34**, 484; https://doi.org/10.1016/j.mencom.2024.06.005.

10 N. B. D. Lima, A. I. S. Silva, S. M. C. Gonçalves and A. M. Simas, *J. Lumin.*, 2016, **170**, 505; https://doi.org/10.1016/j.jlumin.2015.04.044.

11 N. B. D. Lima, A. I. S. Silva, V. F. C. Santos, S. M. C. Gonçalves and A. M. Simas, *RSC Adv.*, 2017, **7**, 20811; https://doi.org/10.1039/C7RA02019H.

12 L. L. L. S. Melo, G. P. Castro, Jr. and S. M. C. Gonçalves, *Inorg. Chem.*, 2019, **58**, 3265; https://doi.org/10.1021/acs.inorgchem.8b03340.

13 N. B. D. Lima, S. M. C. Gonçalves, S. A. Júnior and A. M. Simas, *Sci. Rep.*, 2013, **3**, 2395; https://doi.org/10.1038/srep02395.

14 A. I. S. Silva, V. F. C. Santos, N. B. D. Lima, A. M. Simas and S. M. C. Gonçalves, *RSC Adv.*, 2016, **6**, 90934; https://doi.org/10.1039/C6RA20609C.

15 J. K. Voronina, D. S. Yambulatov, A. S. Chistyakov, A. E. Bolot'ko, L. M. Efromeev, M. A. Shmelev, A. A. Sidorov and I. L. Eremenko, *Crystals*, 2023, **13**, 678; https://doi.org/10.3390/cryst13040678.

16 M. A. Shmelev, A. S. Chistyakov, G. A. Razgonyaeva, J. K. Voronina, E. A. Varaksina, I. V. Taydakov, A. A. Sidorov and I. L. Eremenko, *J. Struct. Chem.*, 2024, **65**, 362; https://doi.org/10.1134/S0022476624020148.

17 M. A. Shmelev, J. K. Voronina, M. A. Evtyukhin, F. M. Dolgushin, E. A. Varaksina, I. V. Taydakov, A. A. Sidorov, I. L. Eremenko and M. A. Kiskin, *Inorganics*, 2022, **10**, 194; https://doi.org/10.3390/inorganics10110194.

18 M. A. Shmelev, G. N. Kuznetsova, N. V. Gogoleva, F. M. Dolgushin, Yu. V. Nelyubina, M. A. Kiskin, A. A. Sidorov and I. L. Eremenko, *Russ. Chem. Bull.*, 2021, **70**, 830; https://doi.org/10.1007/s11172-021-3156-9.

19 M. A. Shmelev, N. V. Gogoleva, V. K. Ivanov, V. V. Kovalev, G. A. Razgonyaeva, M. A. Kiskin, A. A. Sidorov and I. L. Eremenko, *Russ. J. Coord. Chem.*, 2022, **48**, 539; https://doi.org/10.1134/S1070328422090056.

20 R. H. Blessing, *Acta Crystallogr.,* 1995, **A51**, 33; https://doi.org/10.1107/S0108767394005726.

21 O. V. Dolomanov, L. J. Bourhis, R. J. Gildea, J. A. K. Howard and H. Puschmann, *J. Appl. Crystallogr.*, 2009, **42**, 339; https://doi.org/10.1107/S0021889808042726.

22 G. M. Sheldrick, *Acta Crystallogr.*, 2015, **C71**, 3; https://doi.org/10.1107/S2053229614024218.

23 D. Casanova, M. Llunell, P. Alemany and S. Alvarez, *Chem. – Eur. J.*, 2005, **11**, 1479; https://doi.org/10.1002/chem.200400799.

24 P. R. Spackman, M. J. Turner, J. J. McKinnon, S. K. Wolff, D. J. Grimwood, D. Jayatilaka and M. A. Spackman, *J. Appl. Crystallogr.,* 2021, **54**, 1006; https://doi.org/10.1107/S1600576721002910.

25 A. J. Edwards, C. F. Mackenzie, P. R. Spackman, D. Jayatilaka and M. A. Spackman, *Faraday Discuss.*, 2017, **203**, 93; https://doi.org/10.1039/C7FD00072C.

26 A. W.-H. Lam, W. T. Wong, S. Gao, G. Wen and X.-X. Zhang, *Eur. J. Inorg. Chem.*, 2003, **1**, 149; https://doi.org/10.1002/ejic.200390021.

27 M. A. Kiskin, M. A. Shmelev, A. A. Sidorov and I. L. Eremenko, CCDC 2364219: Experimental Crystal Structure Determination, 2024; https://doi.org/10.5517/ccdc.csd.cc2kc548.

28 E. A. Mikhalyova, A. V. Yakovenko, M. Zeller, K. S. Gavrilenko, M. A. Kiskin, S. S. Smola, V. P. Dotsenko, I. L. Eremenko, A. W. Addison and V. V. Pavlishchuk, *Dalton Trans.*, 2017, **46**, 3457; https://doi.org/10.1039/C6DT04757B.

29 M. A. Shmelev, Yu. K. Voronina, N. V. Gogoleva, A. A. Sidorov, M. A. Kiskin, F. M. Dolgushin, Yu. V. Nelyubina, G. G. Aleksandrov, E. A. Varaksina, I. V. Taydakov and I. L. Eremenko, *Russ. Chem. Bull.*, 2020, **69**, 1544; https://doi.org/10.1007/s11172-020-2934-0.

30 M. A. Shmelev, N. V. Gogoleva, A. A. Sidorov, M. A. Kiskin, J. K. Voronina, Yu. V. Nelyubina, E. A. Varaksina, V. M. Korshunov, I. V. Taydakov and I. L. Eremenko, *Inorg. Chim. Acta.*, 2021, **515**, 120050; https://doi.org/10.1016/j.ica.2020.120050.

31 M. H. V. Werts, R. T. F. Jukes and J. W. Verhoeven, *Phys. Chem. Chem. Phys.*, 2002, **4**, 1542; https://doi.org/10.1039/B107770H.

Received: 5th July 2024; Com. 24/7566